Free energy and surface tension of arbitrarily large Mackay icosahedral clusters

Richard B. McClurg and Richard C. Flagan
Division of Chemistry and Chemical Engineering (CN 8723), California Institute of Technology, Pasadena, California 91125

W. A. Goddard III[a)]
Division of Chemistry and Chemical Engineering (CN-8723) and Materials and Molecular Simulation Center, Beckman Institute (139-74), California Institute of Technology, Pasadena, California 91125

(Received 26 August 1994; accepted 11 November 1994)

We present a model for predicting the free energy of arbitrarily large Mackay icosahedral clusters. van der Waals clusters are experimentally observed to be particularly stable at magic numbers corresponding to these structures. Explicit calculations on the vibrational states were used to determine the spectrum of fundamental frequencies for smaller ($\leqslant 561$) icosahedral clusters. The scaled cumulative frequency distribution function rapidly approaches a limiting function for large clusters. This function was used to predict zero-point energies and vibrational free energies for larger clusters (>561 atoms). Combining these predictions with correlations for the moment of inertia and for the minimum potential energy of large clusters leads to free energies of arbitrary large clusters. The free energies are used to predict the chemical potential and surface tension as a function of size and temperature. This connects macroscopic properties to the microscopic atomic parameters. © *1995 American Institute of Physics.*

I. INTRODUCTION

Mass spectroscopic studies on clusters of atoms (Ar,Kr,Xe) and molecules (CO,CH_4) have shown special stability at magic numbers 13, 55, 147, and 309 corresponding to Mackay icosahedral structures.[1] Extensive progress has been made in determining the minimum potential energy configuration of such clusters[2] and it has been shown[3] that Mackay clusters are the minimum potential energy structures for up to about 1600 atoms where decahedral structures become most stable. The bulk (fcc) structure becomes most stable for still larger clusters[3] ($n \approx 10^5$).

Herein we build on such results to predict the free energy of arbitrarily large Mackay icosahedra. This allows us to predict chemical potential $\mu(n)$ for arbitrarily large clusters. Since the slope of μ with respect to $x = n^{-1/3}$ gives the surface tension and the curvature of μ with respect to $x = n^{-1/3}$ gives the Tolman length, this provides a connection between the microscopic parameters (two-body interaction potentials) and macroscopic properties. The predicted values seem consistent with current experimental data. Although the Mackay clusters are not strictly the lowest energy for clusters larger than 1600 atoms, we believe that the resulting surface tension and Tolman length are accurate.

In Sec. II we develop procedures for predicting the free energy as a function of temperature for various Mackay clusters. Free energy calculations for van der Waals clusters have been presented by other authors. The most commonly used atomistic methods fall under two broad categories. Molecular dynamics and Monte Carlo methods confound the various degrees of freedom and hide their functional dependencies which makes extrapolations to larger sizes difficult. Freeman and Doll[4] have reviewed these methods, which will not be discussed further in this paper. In the normal-mode method, several approximations (enumerated below) are used to separate the degrees of freedom into translational, rotational, and vibrational contributions which (as we will show) can each be rationally extrapolated to arbitrarily large sized clusters. Hodgson[5] has summarized much of the previous work using the normal-mode calculation method. The cluster sizes considered previously were limited by the determination of the $(3n-6)$ vibrational frequencies for a cluster containing n atoms. This requires diagonalizing the $3n$ by $3n$ Hessian matrix, which is unwieldy for large clusters. Thus, previous vibrational analyses of physical clusters were limited to Einstein models[6] or to clusters having fewer than 250 atoms.[5] From explicit calculations on up to 561 atoms, we show that the scaled cumulative frequency distributions for progressively larger clusters approach an asymptotic limit. This asymptotic limit permits the rational extrapolation of the vibrational free energy without calculation of the entire set of normal frequencies. The remaining contributions to the free energy will be addressed briefly.

In Sec. III these results are used to predict the surface energy and Tolman length for Ne, Ar, Kr, and Xe.

II. THE FREE ENERGY FUNCTION

A. Structures

The Mackay icosahedral structures[7] are constructed by surrounding a central atom with successively larger icosahedral shells. Each shell maintains icosahedral symmetry with the same orientation of its vertices. The first shell contains 12 atoms at the vertices of the icosahedron. The second shell contains 12 atoms at the vertices plus atoms on each of the 30 edges of the icosahedron for a total of 42 atoms in the second shell and a grand total of 55 atoms. Higher-order

a)To whom correspondence should be addressed.

 0021-9606/95/102(8)/3322/9/$6.00

shells have additional atoms along the edges and in the faces of the icosahedral shell. In general, the number of atoms n in a Mackay structure with N shells is

$$n=1+\sum_{x=1}^{N}(10x^2+2)=\frac{1}{3}(10N^3+15N^2+11N+3). \tag{1}$$

Thus, the first 8 Mackay icosahedral structures contain 13, 55, 147, 309, 561, 923, 1415, and 2057 atoms, respectively. Clusters containing these numbers of atoms are called magic numbered clusters.[8]

TABLE I. Parameters and characteristic quantities for sample systems (Ref. 10). There are two energy scales, D_e and ν_{char}. D_e determines the potential energy at the optimal structure while ν_{char} determines the zero-point energy and vibrational contributions.

Quantity	Units	Ne	Ar	Kr	Xe
m	amu	20.179	39.948	83.80	131.30
D_e	kcal/mol	0.0726	0.237	0.325	0.446
R_e	Å	3.249	3.867	4.109	4.465
$\nu_{\text{char}}=\frac{1}{2\pi R_e}\sqrt{\frac{D_e}{m}}$	GHz	60.12	64.86	49.35	42.50
	cm^{-1}	2.004	2.162	1.645	1.417
$E_{\text{char}}=h\nu_{\text{char}}$	cal/mol	5.729	6.181	4.704	4.051
$T_{\text{char}}=\frac{h\nu_{\text{char}}}{k}$	K	2.883	3.111	2.367	2.039
$I_{\text{char}}=mR_e^2$	amu Å^2	213.0	597.4	1415	2618

B. The free energy

The free energy for an ideal polyatomic gas

$$F=-RT\ln\left(\frac{q}{N_a}\right) \tag{2}$$

is calculated[9] from the single-cluster partition function, q, which can be separated into terms for translation (q_{tr}), rotation (q_{rot}), vibration (q_{vib}), degeneracy (d_j), and a Boltzmann weight

$$q=\sum_j d_j q_{\text{tr}} q_{\text{rot}} q_{\text{vib}} \exp\left(\frac{-E_j}{RT}\right). \tag{3}$$

The degeneracy and Boltzmann weights account for contributions from multiple isomers and are important above the melting temperature of the cluster. They are not needed for the present study which focuses on the solidlike limit.

The partition function is evaluated assuming that the cluster has harmonic vibrations and rotates as a spherically symmetric rigid rotor. Thus

$$q=\sum_j d_j\left[V\left(\frac{2\pi nmkT}{h^2}\right)^{3/2}\right]\left[\left(\frac{\pi^{1/2}}{\sigma_j}\right)\left(\frac{8\pi^2kTI}{h^2}\right)^{3/2}\right] \times\left(\prod_{i=1}^{3n-6}\frac{\exp\left(\frac{-h\nu_i}{2kT}\right)}{1-\exp\left(\frac{-h\nu_i}{kT}\right)}\right)\exp\left(\frac{-E_j}{RT}\right), \tag{4}$$

where m is the mass of each particle, σ is the rotation symmetry number, I is the moment of inertia, V is the volume, k is the Boltzmann constant, R is the gas constant, and h is Planck's constant. We assume that various isomers differ mainly in their degeneracies, binding energies, and symmetry numbers. We assume fixed volume in Eq. (4), thus these results pertain to the low pressure limit.

From Eqs. (2) and (4), the free energy can be written as

$$F=E^{\min}+\sum_{i=1}^{3n-6}\frac{h\nu_i}{2}-RT\ln\left[V\left(\frac{2\pi nmkT}{h^2}\right)^{3/2}\right] -RT\ln\left[\pi^{1/2}\left(\frac{8\pi^2kTI}{h^2}\right)^{3/2}\right] -RT\sum_{i=1}^{3n-6}\ln\left(\frac{1}{1-\exp\left(\frac{-h\nu_i}{kT}\right)}\right) -RT\ln\left[\sum_j\left(\frac{d_j}{\sigma_j}\right)\exp\left(-\frac{E_j-E^{\min}}{RT}\right)\right], \tag{5}$$

where $E^{\min}$ denotes the global minimum potential energy of the cluster.

C. The cumulative frequency function

The interactions among atoms or molecules in the clusters are assumed to involve only two-body interactions. The explicit calculations use the Lennard-Jones potential

$$\epsilon=\rho^{-12}-2\rho^{-6}, \tag{6}$$

$$\epsilon=\frac{E}{D_e}, \tag{7}$$

$$\rho=\frac{r}{R_e}, \tag{8}$$

where r is the distance between the particles. (For molecular clusters multipole electrostatic interactions would also be included.) Energies, temperatures, and vibrational frequencies are nondimensionalized in order for the analysis to be most general. In addition to D_e and R_e, the atomic mass (m) is used to nondimensionalize the data, leading to a characteristic vibrational frequency of

$$\nu_{\text{char}}=\frac{1}{2\pi R_e}\sqrt{\frac{D_e}{m}}. \tag{9}$$

Some typical Lennard-Jones parameters (R_e,D_e) are tabulated[10] in Table I.

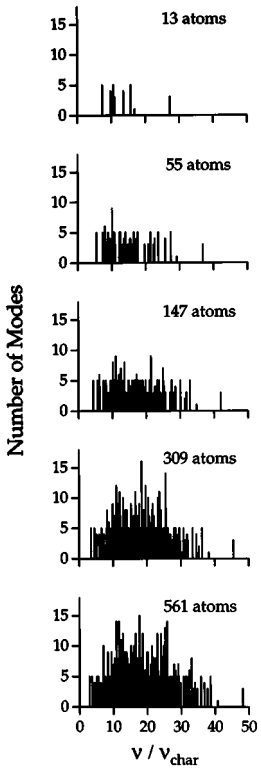

FIG. 1. Histogram of vibrational frequencies for Mackay clusters of 13, 55, 147, 309, and 561 atoms. Frequencies are scaled by the characteristic value $\nu_{\text{char}} = [1/(2\pi R_e)]\sqrt{D_e/m}$. A boxwidth of 0.05 was used in constructing the histogram.

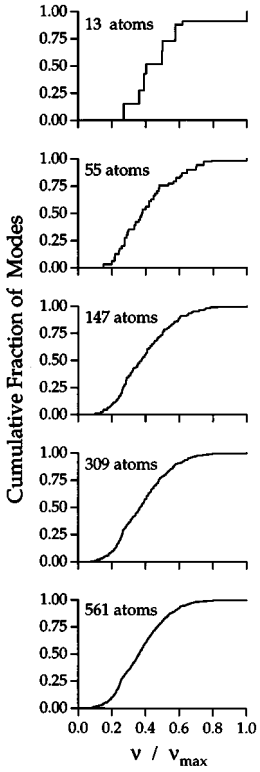

FIG. 2. The cumulative frequency function $[G_N(\nu)]$ for Mackay icosahedral clusters of 13, 55, 147, 309, and 561 atoms. Frequencies are scaled by the largest frequency, ν_{max}, for each cluster. Comparison of $n=147$, 309, and 561 indicates that an asymptotic limit is being reached.

The calculated fundamental vibrational modes and their frequencies are shown in Fig. 1 for icosahedral clusters having 13, 55, 147, 309, and 561 atoms.[11,12] Figure 2 represents this data as the Cumulative Frequency Function, $G_N(\nu)$, for each cluster. The maximum frequency for the cluster (ν_{max}) was used to scale the frequency coordinate and the total number of vibrational modes $(3n-6)$ was used to scale the cumulative modes coordinate. $G_N(\nu)$ appears to approach a smooth, continuous limiting function as $N\rightarrow\infty$.

This observed asymptotic approach to a limiting function for $G_N(\nu)$ is the basis for estimating properties of larger Mackay icosahedral structures. The zero-point energy and heat capacities approach limits as a direct result of $G_N(\nu)$ approaching a limit.

Rather than using $G_N(\nu)$ more typically the vibrational frequencies are expressed in terms of the frequency distribution function, $g_N(\nu)$, defined as the number of normal vibrational frequencies per unit frequency interval,

$$\int_0^{\nu} g_N(x)dx = G_N(\nu). \tag{10}$$

Topological considerations show that for infinite three-dimensional crystals, $g_N(\nu)$ is continuous but with discontinuous slopes (van Hove singularities) arising from long range translational symmetry (the Brillouin zone).[13] The frequency distributions for finite systems differs from the bulk and is sensitive to cluster geometry.[14]

D. Zero-point energy

The zero-point energy for a set of $3n-6$ harmonic oscillators is

$$E^{\text{zp}} = \frac{h}{2}\sum_{i=1}^{3n-6} \nu_i, \tag{11}$$

which can be written in terms of the frequency distribution function, $g(\nu)$,[9]

$$E^{\text{zp}} = \frac{h}{2}\int_0^{\nu_{\text{max}}} \nu g(\nu)d\nu, \tag{12}$$

where $g_N(\nu)$ is zero for $\nu > \nu_{\text{max}}$. We find that ν_{max} is dominated by the motion of the central atom of the cluster moving in the potential of the first (12 atom) shell. The change with N is caused by the compression of this first shell as N is increased. Scaling the frequencies by ν_{char} from Eq. (9) leads to

$$E^{\text{zp}} = \frac{h\nu_{\text{char}}}{2}\int_0^{\hat{\nu}_{\text{max}}} \hat{\nu} g_N(\hat{\nu})d\hat{\nu}, \tag{13}$$

where

$$\hat{\nu} = \frac{\nu}{\nu_{\text{char}}}. \tag{14}$$

Further scaling $g_N(\nu)$ by the total number of frequencies leads to

TABLE II. Calculated and extrapolated maximum frequencies (ν_{max}) and zero-point energies (E^{zp}) for Mackay icosahedral clusters. Frequencies are scaled by the characteristic value ν_{char}, Eq. (9). Zero-point energies are scaled by the characteristic value $E_{char}=h\nu_{char}$. The function J_n is defined in Eq. (17) and fitted by Eq. (18).

		Frequency		Zero point energy		
Shells (N)	Atoms (n)	$\frac{\nu_{max}}{\nu_{char}}$ Calc.	$\frac{E^{zp}}{E_{char}}$ Calc.	J^N Calc.	J^N Extrap.	$\frac{E^{zp}}{E_{char}}$ Extrap.
1	13	27.3	217.5	6.591	6.591	217.5
2	55	36.8	1212	7.623	7.623	1212
3	147	42.0	3600	8.276	8.276	3600
4	309	45.4	7998	8.684	8.684	7998
5	561	48.1	15020	8.956	8.957	15020
6	923				9.151	25280
7	1415				9.296	39410
∞	∞				10.287	

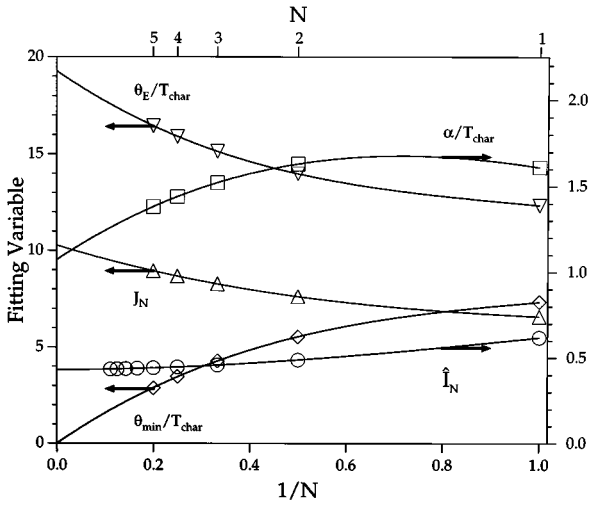

FIG. 3. The five characteristic variables as a function of the number of shells (N) in a cluster: (a) the dimensionless zero-point energy per mode, J_N [see Eq. (17)]; (b) the softening temperature, α [see Eq. (29)]; (c) the characteristic Einstein temperature, θ_E [see Eq. (25)]; (d) the softest mode characteristic temperature, θ_{min} [see Eq. (27)]; and (e) the dimensionless incremental moment of inertia, $\hat{I}_N$ [see Eq. (35)]. All five quantities vary slowly with $1/N$, leading to accurate extrapolations. Zero-point energy is scaled by $E_{char}=(h/2\pi R_e)\sqrt{D_e/m}$. α, θ_E, and θ_{min} are scaled by a characteristic value $T_{char}=h\nu_{char}/k$. The moments are scaled by $I_{char}=mR_e^2$.

$$E^{zp}=(3n-6)h\nu_{char}\int_0^{\hat{\nu}_{max}}\frac{1}{2}\,\hat{\nu}\hat{g}_N(\hat{\nu})d\hat{\nu}, \tag{15}$$

where

$$\hat{g}_N=\frac{g_N}{(3n-6)}. \tag{16}$$

The integral in Eq. (15) is the dimensionless zero-point energy per mode, which we denote as

$$J_N=\frac{1}{2}\int_0^{\hat{\nu}_{max}}\hat{\nu}\hat{g}_N(\hat{\nu})d\nu=\frac{E^{zp}}{(3n-6)h\nu_{char}}. \tag{17}$$

J_N can be calculated from Eq. (17) and the frequency information in Fig. 1. Values for J_N are given in Table II.

Figure 3 shows that the dependence of J_N on the number of filled shells N is quite smooth and well described by the function

$$J_N=10.287-\frac{7.679}{N}+\frac{5.422}{N^2}-\frac{1.439}{N^3}. \tag{18}$$

A Laurent-type expansion is used for fitting throughout this work to avoid nonphysical singularities in the extrapolations to larger clusters. In each case, the order of the fit was chosen to minimize the variance.

E. Vibrational heat capacity

The heat capacity can be written as the sum of contributions from translation, rotation, and vibration

$$C_v=C_v^{tr}+C_v^{rot}+C_v^{vib}. \tag{19}$$

Except for very light clusters at very low temperatures, the translational and rotational contributions are fully classical, leading to

$$C_v=3R+C_v^{vib} \tag{20}$$

(R is the ideal gas constant). We now focus on C_v^{vib}.

The vibrational contribution can be written in terms of a summation over the normal modes as follows:[9]

$$C_v^{vib}=R\sum_{i=1}^{3n-6}\frac{\left(\frac{h\nu_i}{kT}\right)^2\exp\left(\frac{h\nu_i}{kT}\right)}{\left[\exp\left(\frac{h\nu_i}{kT}\right)-1\right]^2}. \tag{21}$$

This leads to a temperature-dependent contribution to the free energy.[9]

$$F^{vib}=RT\sum_{i=1}^{3n-6}\ln\left[1-\exp\left(-\frac{h\nu_i}{kT}\right)\right]. \tag{22}$$

We want to obtain a simple form for F^{vib} containing a small number of independent variables so that the free energy can be estimated without calculating all $(3n-6)$ frequencies.

In the high temperature limit, Eq. (22) can be written as

$$\lim_{T\to\infty}F^{vib}=RT(3n-6)\ln\left[\prod_{i=1}^{3n-6}\left(\frac{h\nu_i}{kT}\right)^{1/(3n-6)}\right]. \tag{23}$$

This is the same limiting behavior as $(3n-6)$ oscillators having an Einstein frequency of

$$\nu_E=\left(\prod_{i=1}^{3n-6}\nu_i\right)^{1/(3n-6)} \tag{24}$$

or an Einstein temperature of

$$\theta_E=\frac{h}{k}\left(\prod_{i=1}^{3n-6}\nu_i\right)^{1/(3n-6)}. \tag{25}$$

Consequently, we fit Eq. (22) with a function

TABLE III. Calculated and extrapolated parameters for fitting the vibrational partition function. Here $\theta_{\min}$ corresponds to the minimum vibrational frequency, θ_E corresponds to the effective Einstein frequency, and α corresponds to the softening frequency. θ_E is defined in Eq. (25) and fitted with Eq. (31). α is defined in Eq. (29) and fitted by Eq. (30). $\theta_{\min}$ is defined in Eq. (27) and fitted with Eq. (32).

Shells (N)	Atoms (n)	$\frac{\alpha}{T_{\text{char}}}$ Fit	$\frac{\alpha}{T_{\text{char}}}$ Extrap.	$\frac{\theta_E}{T_{\text{char}}}$ Calc.	$\frac{\theta_E}{T_{\text{char}}}$ Extrap.	$\frac{\theta_{\min}}{T_{\text{char}}}$ Calc.	$\frac{\theta_{\min}}{T_{\text{char}}}$ Extrap.
1	13	1.61	1.61	12.35	12.35	7.35	7.35
2	55	1.63	1.63	13.98	13.98	5.53	5.54
3	147	1.52	1.52	15.14	15.14	4.29	4.28
4	309	1.44	1.44	15.91	15.92	3.47	3.46
5	561	1.38	1.38	16.46	16.46	2.88	2.89
6	923		1.33		16.85		2.48
7	1415		1.30		17.15		2.17
∞	∞		1.05		19.27		0

$$F^{\text{vib}}=\xi\, RT(3n-6)\ln\left[1-\exp\left(-\frac{\theta_E}{T}\right)\right], \tag{26}$$

where the function $\xi(T)$ has the following characteristics:

$$\xi\sim 1 \quad \text{for } T\to\infty$$

$$\xi\sim\exp\left(\frac{\theta_E-\theta_{\min}}{T}\right) \quad \text{for } T\to 0 \tag{27}$$

$$\theta_{\min}=\frac{h\nu_{\min}}{k}.$$

This accounts for the presence of soft modes which ''freeze out'' at temperatures lower than θ_E. A Padé form consistent with the limiting behavior for ξ is

$$\xi=\exp\left[\left(\frac{\beta+\dfrac{\alpha(\theta_E-\theta_{\min})}{T}}{1+\dfrac{\alpha}{T}}\right)\frac{1}{T}\right]. \tag{28}$$

We find that Eq. (28) with β set to zero is sufficient to accurately fit the full summation in Eq. (22),

$$\xi\approx\exp\left(\frac{\alpha(\theta_E-\theta_{\min})}{T(T+\alpha)}\right). \tag{29}$$

The above analysis reduces the calculation of the vibrational free energy to determining three effective temperatures: α, θ_E, and $\theta_{\min}$. Figure 3 shows that all three vary slowly with $1/N$, leading to accurate extrapolations

$$\frac{\alpha}{T_{\text{char}}}=1.05+\frac{1.97}{N}-\frac{1.88}{N^2}+\frac{0.47}{N^3}, \tag{30}$$

$$\frac{\theta_E}{T_{\text{char}}}=19.27-\frac{16.95}{N}+\frac{15.42}{N^2}-\frac{5.40}{N^3}, \tag{31}$$

$$\frac{\theta_{\min}}{T_{\text{char}}}=0+\frac{17.16}{N}-\frac{14.49}{N^2}+\frac{4.67}{N^3}. \tag{32}$$

The parameters α, θ_E, and $\theta_{\min}$ are listed in Table III for several values of N.

TABLE IV. Moments of inertia for Mackay icosahedral clusters. The moments are scaled by the characteristic value $I_{\text{char}}=mR_e^2$. $\hat{I}_N$ is the scaled incremental moment of inertia given by Eq. (35) and fitted by Eq. (36).

N	n	I/mR_e^2	$\hat{I}_N$
1	13	7.4319	0.6193
2	55	89.431	0.4881
3	147	468.76	0.4581
4	309	1626.6	0.4467
5	561	4406.2	0.4412
6	923	10115	0.4381
7	1415	20627	0.4360
8	2057	38489	0.4347
9	2869	67035	0.4340
∞	∞		0.4257

F. Moment of inertia

Due to the high symmetry of Mackay clusters, the moment of inertia tensor

$$I_{\alpha\beta}=\sum_{j=1}^{n} m_j(\delta_{\alpha\beta}R_j^2-R_{\alpha j}R_{\beta j}) \tag{33}$$

is isotropic, $I_{\alpha\beta}=\delta_{\alpha\beta}I$. The scalar I can be decomposed into contributions from each shell using

$$I=\frac{2}{3}\sum_{y=1}^{N}\sum_{j=1}^{10y^2+2} m_jR_j^2. \tag{34}$$

The average distance R_j is written as $R_j=\rho_j yR_e$ where $\rho_j\approx 1$. Therefore, Eq. (34) becomes

$$\frac{I}{mR_e^2}=\frac{2}{3}\sum_{y=1}^{N}\left[y^2\sum_{j=1}^{10y^2+2}\rho_j\right]=\sum_{y=1}^{N} y^2(10y^2+2)\hat{I}_y, \tag{35}$$

where the function $\hat{I}_N$ is slowly varying and of order one.

The structures for $N=1$ through 9 ($n=13$–2869 atoms) were minimized using POLYGRAF,[11] leading to the results in Table IV and Fig. 3. The following fit to the data is used for extrapolation to larger clusters:

$$\hat{I}_N=0.4298+\frac{0.0104}{N}+\frac{0.2457}{N^2}-\frac{0.0666}{N^3}. \tag{36}$$

G. Minimum potential energy

From explicit calculations on the optimum structures of icosahedral clusters for $N=2$–14 ($n=55$–10179 atoms), Xie *et al.*[15] found that the minimum potential energies can be fitted to the function

$$-\epsilon_N^{\min}=-\frac{E_N^{\min}}{nD_e}=D+Cn^{-1/3}+Bn^{-2/3}+An^{-1} \quad (N>1) \tag{37}$$

with an accuracy of $\pm 0.1D_e$. The expansion coefficients are $A=9.824\ 895\ 8$, $B=1.553\ 495\ 7$, $C=-14.217\ 539$, and $D=8.532\ 635\ 6$.

This data can be reexpressed by an expansion in the number of filled shells,

$$-\epsilon_N^{\min}=-\frac{E_N^{\min}}{nD_e}=\bar{D}+\bar{C}N^{-1}+\bar{B}N^{-2}+\bar{A}N^{-3} \quad (N>1), \tag{38}$$

using $\bar{A}=-1.753\ 665$, $\bar{B}=6.295\ 212$, $\bar{C}=-9.629\ 845$, and $D=8.537\ 573$. Equation (38) is more useful in the current context since it expresses the minimum potential energy as an expansion in the same independent variable as for the other functions.

For the single shell case ($n=13$)

$$-\epsilon_1^{\min}=3.410. \tag{39}$$

H. Symmetry numbers, degeneracies, and isomers

For icosahedral clusters, the rotational symmetry number (σ) is 60 and the degeneracy (d) is 1. Other isomers will tend to have symmetry numbers of order one, but higher degeneracies. Although these factors would tend to favor other isomers in the partition function, the Boltzmann weighting ensures that the icosahedral structure is dominant until the temperature is comparable[16] to $0.3D_e/R$. Above this temperature, the cluster surface melts and multiple inherent structures become significant. We consider this melting temperature as the upper limit for application of our model.

I. Summary

The correlations presented in Eqs. (18), (30)–(32), (36), and (38) can now be used to predict the free energies of arbitrarily large magic-numbered Mackay icosahedral clusters

$$F=nD_e\epsilon_N^{\min}+(3n-6)h\nu_{\text{char}}J_N-RT\ \ln\left[V\left(\frac{2\pi nmkT}{h^2}\right)^{3/2}\right]$$
$$-RT\ \ln\left[\pi^{1/2}\left(\frac{8\pi^2kTmR_e^2}{h^2}\sum_{y=1}^{N}y^2(10y^2+2)\hat{I}_y\right)^{3/2}\right]$$
$$+RT(3n-6)\left\{\ln\left[1-\exp\left(-\frac{\theta_E}{T}\right)\right]\right\}$$
$$\times\exp\left[\frac{\theta_E-\theta_{\min}}{T\left(1+\frac{T}{\alpha}\right)}\right]+RT\ \ln 60. \tag{40}$$

III. DISCUSSION

The above derivation assumes that the atoms or molecules vibrate around some equilibrium position. That is, the clusters are solidlike. In addition the vibrational partition function was analyzed assuming all vibrational states are harmonic oscillators. The anharmonicity will influence the heat capacity, particularly at higher temperatures.

Above the melting temperature, multiple isomeric structures become significant. Calculations by Honeycutt and Andersen[16] on 13 and 55 atom clusters suggest that melting occurs at a temperature between $0.3D_e/R$ and $0.4D_e/R$. Thus, the vibrational contribution to the free energy in Eq. (26) is a low temperature approximation, with large deviations expected as the melting point is reached.

Our predictions for $N\rightarrow\infty$ are restricted to Mackay icosahedra. For sufficiently large N the most stable structure is the face centered cubic (fcc) crystalline form. Indeed for Lennard-Jones clusters, a decahedral structure becomes stable above 1600 atoms.[3] Even so, it is of interest to examine the properties predicted for infinite systems from these calculations because this allows a connection between macroscopic properties and microscopic parameters (R_e,D_e,m).

A. Bulk properties—classical analysis

We will use several equations from macroscopic thermodynamics to relate cluster-free energies to bulk chemical potentials and surface tensions. The free energy of a macroscopic liquid drop (F) can be written in terms of the number of particles in the drop (n), the chemical potential of a particle in the bulk (μ), the surface area of the drop (a), and the surface tension (σ)

$$F=n\mu+a\sigma. \tag{41}$$

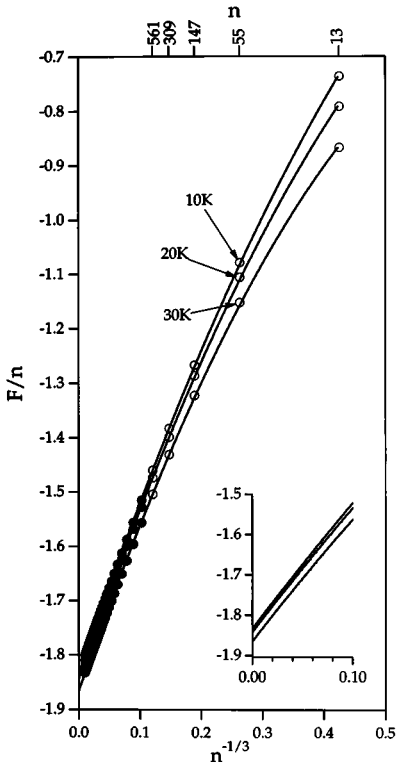

FIG. 4. Calculated free energy per particle vs $n^{-1/3}$ for argon as motivated by Eq. (45). The intercept is the bulk chemical potential, the slope at the origin is related to the surface tension, and the curvature is related to the Tolman length. Unfilled circles are from explicit calculations, while filled ones are from extrapolations.

TABLE V. The bulk chemical potential (μ), surface tension (σ), and Tolman length (δ) for the solid form of four noble gases, estimated using Eq. (45). For the 0 K evaluations, the temperature-dependent contributions to the free energy were set to zero.

Solid	T (K)	μ $\left(\frac{\text{kcal/mol}}{\text{particle}}\right)$	σ $\left(\frac{\text{dyn}}{\text{cm}}\right)$	δ (Å)
Ne	0	−0.443	15.9	0.44
	10	−0.444	16.0	0.60
Ar	0	−1.834	42.1	0.46
	10	−1.834	42.2	0.52
	20	−1.843	42.0	0.59
	30	−1.866	41.5	0.66
Kr	0	−2.631	52.5	0.48
	10	−2.633	52.6	0.53
	20	−2.648	52.3	0.58
	30	−2.681	51.8	0.64
	40	−2.730	51.2	0.70
Xe	0	−3.684	61.8	0.51
	10	−3.687	61.9	0.55
	20	−3.707	61.6	0.60
	30	−3.746	61.2	0.65
	40	−3.803	60.7	0.69
	50	−3.873	60.1	0.74
	60	−3.954	59.5	0.78

Tolman showed[17] that the surface tension of a spherical drop is related to the radius of curvature (r) as in

$$\sigma(r)=\sigma_0\left(1-\frac{2\delta}{r}\right)+0(r^{-2}). \tag{42}$$

Although Eq. (42) is only the lowest-order correction, we will use the Tolman length (δ) as a fitting parameter down to the smallest Mackay clusters. For spherical drops, the surface area, radius of curvature, and number of particles are related through the molecular volume (v)

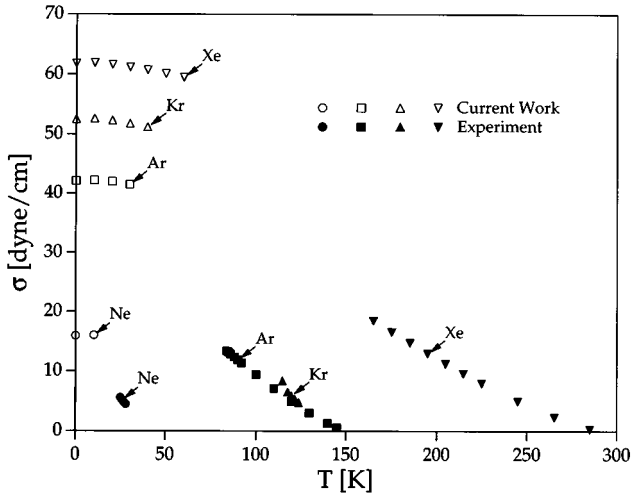

FIG. 5. Calculated and experimental (Refs. 18 and 19) surface tension for four noble gases. The calculated values (open symbols) are for the solid while the experimental values (filled symbols) are for the liquid.

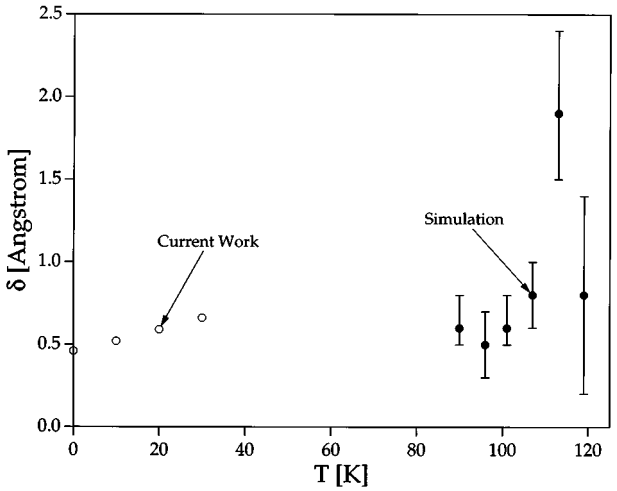

FIG. 6. Calculated (present work) and simulated (Ref. 20) (using molecular dynamics) Tolman length for argon. The error bars on the simulation results are $\pm 1\sigma$.

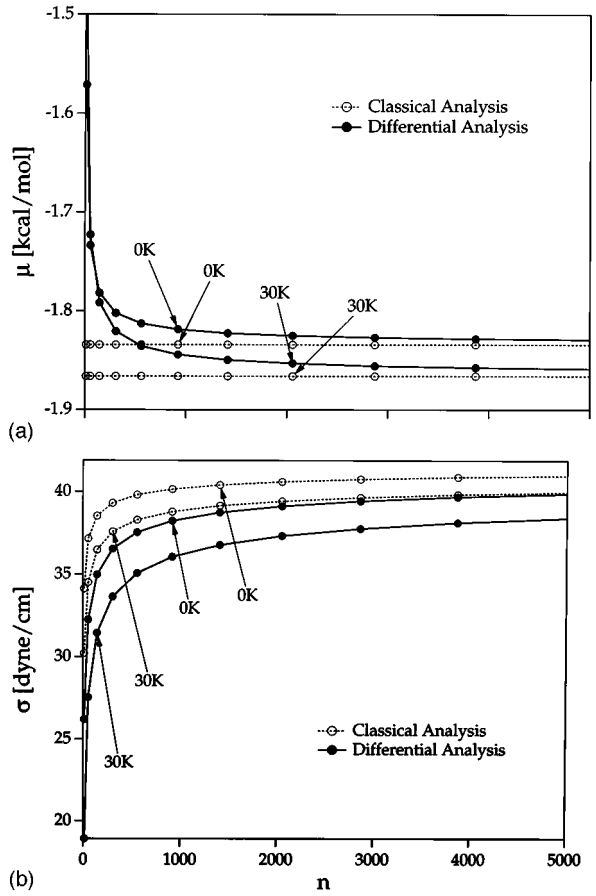

FIG. 7. (a) The bulk chemical potential for solid argon using the classical analysis (dashed lines) and the differential analysis (solid lines). The classical approach assumes that the bulk chemical potential is size independent. (b) The surface tension for solid argon using the classical analysis (dashed lines) and the differential analysis (solid lines).

TABLE VI. Calculated chemical potential (μ), surface tension (σ), and free energy (F/n) as functions of the number of atoms (n) in a cluster using the classical analysis.

Solid	T (K)	v $\left(\frac{\text{Å}^3}{\text{particle}}\right)$	μ $\left(\frac{\text{kcal}}{\text{mol}}\right)$	σ $\left(\frac{\text{dyn}}{\text{cm}}\right)$	F/n $\left(\frac{\text{kcal/mol}}{\text{particle}}\right)$
Ne	0	22.184	-0.443	$15.9-7.984n^{-1/3}$	$-0.443+0.874n^{-1/3}-0.439n^{-2/3}$
	10	22.184	-0.444	$16.0-10.945n^{-1/3}$	$-0.444+0.879n^{-1/3}-0.602n^{-2/3}$
Ar	0	37.465	-1.834	$42.1-18.643n^{-1/3}$	$-1.834+3.277n^{-1/3}-1.453n^{-2/3}$
	10	37.465	-1.834	$42.2-21.124n^{-1/3}$	$-1.834+3.287n^{-1/3}-1.647n^{-2/3}$
	20	37.465	-1.843	$42.0-23.911n^{-1/3}$	$-1.843+3.272n^{-1/3}-1.864n^{-2/3}$
	30	37.465	-1.866	$41.5-26.554n^{-1/3}$	$-1.866+3.235n^{-1/3}-2.070n^{-2/3}$
Kr	0	45.019	-2.631	$52.5-22.691n^{-1/3}$	$-2.631+4.622n^{-1/3}-1.999n^{-2/3}$
	10	45.019	-2.633	$52.6-25.126n^{-1/3}$	$-2.633+4.630n^{-1/3}-2.214n^{-2/3}$
	20	45.019	-2.648	$52.3-27.703n^{-1/3}$	$-2.648+4.605n^{-1/3}-2.441n^{-2/3}$
	30	45.019	-2.681	$51.8-30.124n^{-1/3}$	$-2.681+4.560n^{-1/3}-2.654n^{-2/3}$
	40	45.019	-2.730	$51.2-32.430n^{-1/3}$	$-2.730+4.508n^{-1/3}-2.858n^{-2/3}$
Xe	0	57.661	-3.684	$61.8-26.439n^{-1/3}$	$-3.684+6.424n^{-1/3}-2.748n^{-2/3}$
	10	57.661	-3.687	$61.9-28.641n^{-1/3}$	$-3.687+6.431n^{-1/3}-2.976n^{-2/3}$
	20	57.661	-3.707	$61.6-30.899n^{-1/3}$	$-3.707+6.401n^{-1/3}-3.211n^{-2/3}$
	30	57.661	-3.746	$61.2-33.020n^{-1/3}$	$-3.746+6.354n^{-1/3}-3.432n^{-2/3}$
	40	57.661	-3.803	$60.7-35.042n^{-1/3}$	$-3.803+6.300n^{-1/3}-3.642n^{-2/3}$
	50	57.661	-3.873	$60.1-36.994n^{-1/3}$	$-3.873+6.242n^{-1/3}-3.844n^{-2/3}$
	60	57.661	-3.954	$59.5-38.894n^{-1/3}$	$-3.954+6.181n^{-1/3}-4.042n^{-2/3}$

$$a=4\pi r^2, \tag{43}$$

$$nv=\tfrac{4}{3}\pi r^3. \tag{44}$$

Using Eqs. (41)–(44), the free energy of the drop can be written as a power series in $n^{-1/3}$

$$\frac{F}{n}=\mu+\sigma_0(4\pi)^{1/3}(3v)^{2/3}n^{-1/3}-2\sigma_0\delta(4\pi)^{2/3}(3v)^{1/3}n^{-2/3}. \tag{45}$$

Figure 4 shows a plot of the free energy per particle (F/n) for argon clusters vs $n^{-1/3}$ for three temperatures.

TABLE VII. Calculated chemical potential (μ), surface tension (σ), and free energy (F/n) as functions of the number of atoms (n) in a cluster using the differential analysis.

Solid	T (K)	v $\left(\frac{\text{Å}^3}{\text{particle}}\right)$	μ $\left(\frac{\text{kcal}}{\text{mol}}\right)$	σ $\left(\frac{\text{dyn}}{\text{cm}}\right)$	F/n $\left(\frac{\text{kcal/mol}}{\text{particle}}\right)$
Ne	0	22.184	$-0.443+0.439n^{-2/3}$	$15.9-2*7.984n^{-1/3}$	$-0.443+0.874n^{-1/3}-0.439n^{-2/3}$
	10	22.184	$-0.444+0.602n^{-2/3}$	$16.0-2*10.945n^{-1/3}$	$-0.444+0.879n^{-1/3}-0.602n^{-2/3}$
Ar	0	37.465	$-1.834+1.453n^{-2/3}$	$42.1-2*18.643n^{-1/3}$	$-1.834+3.277n^{-1/3}-1.453n^{-2/3}$
	10	37.465	$-1.834+1.647n^{-2/3}$	$42.2-2*21.124n^{-1/3}$	$-1.834+3.287n^{-1/3}-1.647n^{-2/3}$
	20	37.465	$-1.843+1.864n^{-2/3}$	$42.0-2*23.911n^{-1/3}$	$-1.843+3.272n^{-1/3}-1.864n^{-2/3}$
	30	37.465	$-1.866+2.070n^{-2/3}$	$41.5-2*26.554n^{-1/3}$	$-1.866+3.235n^{-1/3}-2.070n^{-2/3}$
Kr	0	45.019	$-2.631+1.999n^{-2/3}$	$52.5-2*22.691n^{-1/3}$	$-2.631+4.622n^{-1/3}-1.999n^{-2/3}$
	10	45.019	$-2.633+2.214n^{-2/3}$	$52.6-2*25.126n^{-1/3}$	$-2.633+4.630n^{-1/3}-2.214n^{-2/3}$
	20	45.019	$-2.648+2.441n^{-2/3}$	$52.3-2*27.703n^{-1/3}$	$-2.648+4.605n^{-1/3}-2.441n^{-2/3}$
	30	45.019	$-2.681+2.654n^{-2/3}$	$51.8-2*30.124n^{-1/3}$	$-2.681+4.560n^{-1/3}-2.654n^{-2/3}$
	40	45.019	$-2.730+2.858n^{-2/3}$	$51.2-2*32.430n^{-1/3}$	$-2.730+4.508n^{-1/3}-2.858n^{-2/3}$
Xe	0	57.661	$-3.684+2.748n^{-2/3}$	$61.8-2*26.439n^{-1/3}$	$-3.684+6.424n^{-1/3}-2.748n^{-2/3}$
	10	57.661	$-3.687+2.976n^{-2/3}$	$61.9-2*28.641n^{-1/3}$	$-3.687+6.431n^{-1/3}-2.976n^{-2/3}$
	20	57.661	$-3.707+3.211n^{-2/3}$	$61.6-2*30.899n^{-1/3}$	$-3.707+6.401n^{-1/3}-3.211n^{-2/3}$
	30	57.661	$-3.746+3.432n^{-2/3}$	$61.2-2*33.020n^{-1/3}$	$-3.746+6.354n^{-1/3}-3.432n^{-2/3}$
	40	57.661	$-3.803+3.642n^{-2/3}$	$60.7-2*35.042n^{-1/3}$	$-3.803+6.300n^{-1/3}-3.642n^{-2/3}$
	50	57.661	$-3.873+3.844n^{-2/3}$	$60.1-2*36.994n^{-1/3}$	$-3.873+6.242n^{-1/3}-3.844n^{-2/3}$
	60	57.661	$-3.954+4.042n^{-2/3}$	$59.5-2*38.894n^{-1/3}$	$-3.954+6.181n^{-1/3}-4.042n^{-2/3}$

Quadratic fits to the data yield estimates of three of the four material properties in Eq. (45). Assuming the bulk density of the solid[10] as the fourth parameter allows the bulk chemical potential, surface tension, and Tolman length to be calculated. The results of these calculations are in Table 5. Figure 5 shows that the predicted surface energies at low temperature are in good qualitative agreement with published measurements for higher temperatures.[18,19] In addition, Fig. 6 shows good agreement of the predicted Tolman lengths with the results of recent molecular dynamics simulations of a liquid/vapor interface for a Lennard-Jones fluid.[20] Such agreement lends support for using the extrapolations on Mackay icosahedral clusters even though they are not the lowest energy structures for clusters containing more than 1600 particles. The close relationship between Mackay icosahedral structures and fcc structures[7] may aid in the extrapolation. Nevertheless, these predictions are seen as confirmation of the extrapolation procedure presented herein.

Figure 7 shows the size dependence of the bulk chemical potential and surface tension for argon. Table 6 gives expressions for the bulk chemical potential and surface tension for Ne, Ar, Kr, and Xe at several temperatures. It is inherent in the classical approach that the chemical potential is independent of size.

B. Bulk properties—differential analysis

An alternative to the above analysis is to use a size-dependent bulk chemical potential (rather than a constant). Thus from Fig. 4, the slope $[f'(x)]$ and intercept $[f(x)]$ of the tangent line at a given $x=n^{-1/3}$ are used to define the effective bulk chemical potential (μ) and surface tension (σ), respectively,

$$\mu = f(x), \tag{46}$$

$$\sigma(4\pi)^{1/3}(3v)^{2/3} = f'(x), \tag{47}$$

where

$$x = n^{-1/3} \tag{48}$$

and

$$f = \frac{F}{n}. \tag{49}$$

Figure 7 shows the size dependence of the effective bulk chemical potential and surface tension using the differential analysis for argon. Table 7 gives expressions for the bulk chemical potential and surface tension for Ne, Ar, Kr, and Xe at several temperatures.

Since the classical and differential methods use the same quadratic fits to the free energy data, they contain the same information. The classical approach has the advantage of being simpler, but the differential approach provides additional physical insight. Due to the proximity of the surface, none of the atoms in nanoscale clusters are in a bulk environment. In the classical analysis, these surface effects are ''lumped'' in with the size dependence of the surface tension while the bulk chemical potential is fixed. In the differential analysis, the chemical potential of the interior atoms approaches the bulk value as the surface becomes sufficiently distant. Future analyses may benefit from explicitly handling the size dependence of the bulk chemical potential in this manner.

ACKNOWLEDGMENTS

We thank Dr. Guanhua Chen for helpful discussions, Dr. Terry Coley for assistance with the vibrational calculations on large systems, and Dr. Siddharth Dasgupta for modifications to POLYGRAF. R.B M. acknowledges a National Science Foundation Graduate Research Fellowship. Partial support of the work was provided by grants from the NSF (Nos. CHE 91-100289, CTS 91-13191, and ASC 9217368). The computer facilities of the MSC used in this work are also supported by grants from DOE-AICD, Allied-Signal Corp., Asahi Chemical, Asahi Glass, BP America, Chevron, BF Goodrich, Teijin Ltd., Vestar, Hughes Research Laboratories, Xerox, and Beckman Institute.

[1] O. Echt, O. Kandler, T. Leisner, W. Miehle, and E. Recknagel, J. Chem. Soc. Faraday Trans. **86**, 2411 (1990), and references therein.
[2] J. A. Northby, J. Chem. Phys. **87**, 6166 (1987), and references therein.
[3] B. Raoult, J. Farges, M. F. DeFeraudy, and G. Torschet, Phil. Mag. B **60**, 881 (1989), and references therein.
[4] D. L. Freeman and J. D. Doll, Adv. Chem. Phys. **70B**, 139 (1988).
[5] A. W. Hodgson, Adv. Colloid Interface Sci. **21**, 303 (1984), and references therein.
[6] F. F. Abraham, and J. V. Dave, J. Chem. Phys. **55**, 4817 (1971).
[7] A. L. Mackay, Acta Cryst. **15**, 916 (1962).
[8] R. F. K. Herzog, W. P. Poschenrieder, and F. G. Satkiewicz, Radiat. Effects **18**, 199 (1973).
[9] T. L. Hill, *Statistical Thermodynamics* (Dover, New York, 1986), pp. 98–100, 161–167.
[10] The Lennard-Jones parameters used in this study were chosen to agree with the bulk lattice spacing [J. Donohue, *Structures of the Elements* (Krieger, Malabar, FL, 1982)] and the heat of vaporization at 0 K after correcting for zero point energy [R. Hultgren *et al.*, *Selected Values of the Thermodynamic Properties of the Elements* (American Society for Metals, Metals Park, OH, 1973)]. The method used to calculate Lennard-Jones parameters from this information is detailed elsewhere [N. Karasawa and W. A. Goddard III, J. Phys. Chem. **93**, 7320 (1989)].
[11] The coordinates of the atoms in the minimized structures and the vibrational frequencies were determined using POLYGRAF (Ref. 12) from Molecular Simulations Inc (Burlington, Mass).
[12] A fast routine written by Dr. Terry Coley was used to determine the frequencies for the 561-atom cluster.
[13] L. V. Hove, Phys. Rev. **89**, 1189 (1953).
[14] J. M. Dickey and A. Paskin, Phys. Rev. B **1**, 851 (1970).
[15] J. Xie, J. A. Northby, L. Freeman, and J. D. Doll, J. Chem. Phys. **91**, 612 (1989).
[16] J. D. Honeycutt and H. C. Andersen, J. Phys. Chem. **91**, 4950 (1987).
[17] R. C. Tolman, J. Chem. Phys. **17**, 333 (1949).
[18] J. L. Jasper, J. Phys. Chem. Ref. Data **1**, 841 (1972).
[19] G. A. Cook, *Argon, Helium, and the Rare Gases* (Interscience, New York, 1961).
[20] M. J. Haye and C. Bruin, J. Chem. Phys. **100**, 556 (1994).